η^3

NACA

RESEARCH MEMORANDUM

EXPERIMENTAL INVESTIGATION OF AIR-SIDE PERFORMANCE

OF LIQUID-METAL TO AIR HEAT EXCHANGERS

By Louis Gedeon, Charles W. Conant, and Samuel J. Kaufman

Lewis Flight Propulsion Laboratory
Cleveland, Ohio

CLASSIFICATION CHANGED

UNCLASSIFIED

To _____

By authority of *JPa #33* Date *10-28-61*

um

NATIONAL ADVISORY COMMITTEE
FOR AERONAUTICS
WASHINGTON
March 16, 1956

NASA Technical Library

3 1176 01435 4568

3914

NATIONAL ADVISORY COMMITTEE FOR AERONAUTICS

RESEARCH MEMORANDUM

EXPERIMENTAL INVESTIGATION OF AIR-SIDE PERFORMANCE

OF LIQUID-METAL TO AIR HEAT EXCHANGERS

By Louis Gedeon, Charles W. Conant, and Samuel J. Kaufman

SUMMARY

Heat-transfer and pressure-drop data were experimentally obtained for the air side of a liquid-metal to air, shell-and-tube heat exchanger. Tests were conducted in a 500 kilowatt facility using sodium as the shell-side heating fluid. Because of weld failures, only isothermal-pressure-drop data for a finned-tube heat exchanger are included. Exchanger-inlet-air temperature was varied from 70° to 600° F for Reynolds numbers of 7000 to 115,000. Average inlet sodium temperatures were maintained between 800° and 1100° F.

Air-side heat-transfer data for the shell-and-tube heat exchanger were correlated by the familiar Nusselt relation corrected for length-to-diameter ratio. Tests were run with sodium having a relative large amount of oxygen and with sodium having a reduced oxygen content. The latter gave results that were in good agreement with the recommended line.

Pressure-drop data for the shell-and-tube heat exchanger were compared with the Kármán-Nikuradse relation for friction factor and Reynolds number. Isothermal data and low Reynolds number data with heat transfer gave good agreement with the recommended line. High Reynolds number data with heat transfer gave a friction factor that fell considerably below the line. Isothermal-pressure-drop data for a finned-tube heat exchanger were compared with an analytical investigation for flat plates and found to be 55 percent higher than predicted by the analysis for flat plates.

INTRODUCTION

A 500-kilowatt test facility for use in evaluating the performance of liquid-metal to air heat exchangers has been constructed at the NACA Lewis laboratory. This report describes the test facility and presents data obtained for two heat exchangers.

The first heat exchanger tested is the conventional shell-and-tube type with sodium as the shell fluid. Heat is transferred to the air flowing through the tubes. This type of exchanger was selected for the initial tests because of ease of fabrication.

The second heat exchanger built was of the finned-tube type, in which sodium flowed through the tubes while air flowed over the fins and banks of tubes. Because of weld failures, only isothermal-pressure-drop data is reported for the finned-tube heat exchanger.

The 500-kilowatt facility is designed so that flight conditions at Mach 1.5 at an altitude of 30,000 feet with a compressor pressure ratio of 7.0 can be simulated. In addition, varying the inlet-air temperature and pressure allows testing at other flight conditions. Maximum operating conditions for the loop are as follows:

Air flow, lb/sec 4
Inlet-air temperature, °F 700
Sodium flow, lb/sec 6
Inlet sodium temperature, °F 1500
Heat-transfer rate, Btu/sec 475

The data reported herein were obtained over a range of each of the operating variables.

Additional heat exchangers of varied design are being constructed for test. The ultimate goal is to determine which liquid-metal to air heat exchanger best fulfills the following requirements for nuclear-powered aircraft:

(1) High-thermal efficiency

(2) Low air-side pressure drop

(3) Low weight

(4) Ease of fabrication

(5) Reliability

APPARATUS

A schematic diagram of the test facility is shown in figure 1. Sodium is circulated from the sump tank by a vertical shaft centrifugal pump through the electric-resistance heater, heat exchanger, volume measuring tank, and back to the sump tank. The sodium loop is designed to drain by gravity into the sump tank.

Regulating valves, orifice, fuel burner, mixing baffles, and straightening vanes make up the air side of the system. Proper heat-exchanger-inlet-air conditions are set by positioning the throttling valves and adjusting the fuel flow to the burner.

Test Facility

Details of the various components of the test facility are given in the following paragraphs.

Sump tank. - The sump tank is constructed of AISI 300 series stainless steel, 36 inches in diameter and 33 inches deep. The wall is made of a 3/8-inch plate, the bottom is a 1/2-inch plate, and a 3/4-inch cover plate supports the centrifugal pump. About 500 pounds of sodium are contained in the sump tank. Originally oil-pumped nitrogen gas was used as a blanket over the sodium surface. Because the oxygen content of the nitrogen was greater than expected, argon was substituted. In order to insure that a minimum of oxygen is introduced into the system, the argon gas is further purified by bubbling it through two tanks of liquid sodium-potassium alloy.

Sump pump. - A vertical shaft centrifugal pump circulates liquid sodium through the loop. At a rated speed of 1800 rpm, the pump capacity is 50 gpm. Since the pump shaft, housing, impeller, and supports are immersed in sodium they are made of stainless steel. The bearings and shaft supports are located above the sump tank. An air-cooled graphite-impregnated asbestos seal mounted on the cover plate is used to prevent gas leakage around the pump shaft. A labyrinth-type slinger ring is fastened to the pump shaft to minimize sodium leakage.

The pump is belt driven by a 30-horsepower variable-speed direct-current motor which is powered and controlled by a motor-generator set.

Electric-resistance heater. - In order to obtain a desired sodium temperature, heat is added in the electric-resistance heater. AISI type 304 stainless-steel tubing, 30 feet long, $1\frac{1}{4}$ inches in diameter with a 0.125-inch wall, is bent in a double return section (fig. 1). The hot bus-bar connection is at the midpoint and the end points are at ground potential to restrict the electric current flow to the heater section. Since sodium is an electric conductor, heat is generated in the sodium flowing through the heater as well as in the pipe. The main heater is encased in a transite box packed with magnesia insulation.

Electric system. - Electric power from a 2400 volt, 60 cycle line is supplied to the main heater through a power transformer. The power is controlled by a saturable reactor on the primary side of the transformer. An air-cooled coaxial bus bar connects the transformer to the

main heater. The capacity of the electric system is 500 kilowatts at a
maximum of 25 volts across the main heater. Volts, amperes, and watts
are read on the transformer secondary. Current is measured by the use
of a 20,000/5 ampere current transformer.

Volume measuring tank. - The volume measuring tank is constructed
of 3/8-inch stainless steel, 18 inches in diameter, and 30 inches deep.
A plunger-type valve actuated by an air-driven piston closes the exit
line at the bottom of the tank. Three electric contact points insulated
from the tank are installed at known depths. An electric stopclock is
actuated by the sodium making contact with the lowest contact point. Upon
reaching the middle or highest contact the clock is stopped and the drain
valve opens. A thermocouple located inside the tank indicates the so-
dium temperature. With the time required to fill a designated volume and
the density of sodium at the recorded temperature given, the sodium flow
rate is determined. A sieve-type splash guard located above the sodium
entrance maintains a level surface.

An overflow line runs from the top of the volume measuring tank to
the sump tank. Two functions of this line are (1) sodium is allowed to
flow back into the sump tank in the event the plunger valve fails to
open, and (2) it serves as a vent line when the volume tank is being
filled.

Piping and preheaters. - All piping between elements is $1\frac{1}{2}$-inch
stainless-steel tubing. Ring-joint flanges are used for easy disassembly.
To eliminate the possibility of leaks, extreme care is taken in the
alinement of the flanges. The flanges are neither preheated nor insulated
to reduce the probability of the bolts expanding and therefore loosening
the connection.

Nichrome V heating wire threaded in ceramic beads and wrapped around
each element of the sodium loop serve as preheaters to bring the system
up to temperature. Power is supplied to each heater by a variable
transformer.

Filter tank. - In order to charge the loop, sodium is first melted
in the filter tank, and then argon pressure is used to force the liquid
sodium through a 5-micron micrometallic filter into the sump tank. The
filter tank is used, periodically, to keep the sodium oxide content to
a minimum. In this process the sump tank is heated to 1000° F. Sodium
is then transferred to the filter tank where it cools to about 300° F.
Sodium oxide precipitates out and the filtered sodium is returned to the
sump tank.

3914

Air tunnel. - Air-flow rates and pressures are regulated by control valves located before and after the heat exchanger. A maximum air-flow rate of 4 pounds per second is available at a pressure of 120 pounds per square inch. The air-flow rate is measured by a standard sharp-edge orifice in a 6-inch line. The air is heated to a desired temperature by an altered J-35 burner-can assembly. The air then flows through a set of mixing baffles, straightening vanes, a bellmouthed-entrance section and into the test section from which it is exhausted to the atmosphere through a muffler. Total-temperature, total-pressure, and static-pressure measurements are taken before and after the heat exchanger.

Temperature and pressure measurements. - Air-inlet and -outlet and sodium-inlet and -outlet temperatures are measured by means of chromel-alumel thermocouples. In addition to these, each section of pipe is spotted with chromel-alumel thermocouples of 24 gage. All temperatures are read on a self-balancing, indicating-type potentiometer. A rake made up of nine total-temperature thermocouples and nine total-pressure tubes is located before and after the heat exchanger. The thermocouples and pressure tubes are positioned in the center of three equal concentric areas for the shell-and-tube heat exchanger and the center of nine equal rectangular areas for the finned-tube heat exchanger. Four static-pressure taps are located on the tunnel wall in the same plane as the total-pressure tubes. Total and static pressures are indicated on banks of mercury manometers which are photographed for each run in order to simplify the recording of data and to provide a permanent record.

Safety devices. - Thermocouples attached to cutout switches·are used to detect

(1) Overtemperature of main heater

(2) Overtemperature of sump tank

(3) Overtemperature of burner-outlet air

(4) Undertemperature of sump tank

(5) Undertemperature of burner-outlet air

Any of these will shut down the system. Insufficient bus-bar cooling air and pump speed will also shut down the system.

A sodium leak and flame detector designed at NACA is also employed in this system. This unit is immediately downstream of the heat exchanger. Both the flame- and leak-detecting units use photoelectric tubes in conjunction with filters that absorb all light except the spectral line of burning sodium. The flame detector is located on the tunnel wall and sees all the exchanger-exit air. The leak-detecting unit views a sample of exchanger-outlet air that is passed over a bunsen flame. A sodium fire in the air tunnel or at the Bunsen burner will shut down the system.

Shell-and-tube heat exchanger. - The first heat exchanger tested in
this loop is of the shell-and-tube design (fig. 2). Sodium flows in the
shell over the bundle of tubes as the air passes counterflow through the
tubes. The sodium side has 3 baffles extending slightly past the center
of the shell making a crossflow-counterflow arrangement. The shell is
constructed of 1/8-inch AISI 300-series stainless-steel plate, 29 inches
long and 4.25 inches in diameter. The ring around the shell shown in
figure 2(b) is an expansion joint.

A total of 241 tubes, 28 inches long, are spaced in a triangular
array on 1/4-inch centers. A closeup photograph of the header and tubes
is shown in figure 2(c). The stainless-steel tubes, which are 3/16 inch
in outside diameter with a 0.016-inch wall are heliarc welded to 1/8-
inch header plates.

Since sodium is one of the exchanger fluids, extreme care was taken
in all welds. The exchanger was pressure checked to find any large leaks.
In order to locate the smaller leaks that cannot be detected by a pres-
sure check, a mass-spectrometer-type leak detector was used.

Finned-tube heat exchanger. - The finned-tube heat exchanger is
shown in figure 3. Sodium flows through 102 3/16-inch outside diameter
tubes, which have 0.016-inch walls, arranged to form a two-pass crossflow
heat exchanger. The tubes are in a staggered array with three tubes in
each bank and a half round against the exchanger wall. Plates, 0.020
inch thick and 28 inches long, were drilled, dimpled, and press fitted
over the 102 tubes. There are 77 fins giving a spacing between fins of
about 0.032 inch. The sides and header are made of a 1/8-inch plate.
All components are made of AISI 300-series stainless steel. This ex-
changer was also thoroughly tested for leaks.

TEST PROCEDURE

Pressure-drop data were taken with and without heat addition. For
the isothermal conditions, the air-flow rate is set and preheated to a
desired temperature level. After equilibrium is reached, flow rate,
pressures, and temperatures are recorded. The flow rate is varied from
0.5 to 3 pounds per second for a range of exchanger-inlet-air tempera-
tures from 70° to 600° F.

The following general procedure is used to obtain experimental data
with heat transfer. Using the preheaters, the entire sodium loop is
heated to about 300° F with the exception of the sump tank which is
brought up to 650° F. Heating the sodium to this higher temperature as-
sures flow through cold areas such as the flanges which are not preheated.
Air-flow rate and temperature are set. The sodium pump is started and
its speed is adjusted to give a flow of about 5 pounds per second. The

main heater power supply is turned on to bring the sodium temperature to above 800° F. The electric power is then adjusted to balance the heat transferred to the air and surroundings. After equilibrium conditions are obtained, power input, flow rates, pressures, and temperatures are recorded.

The air-flow rate is changed in suitable increments ranging from 0.5 to 3 pounds per second for exchanger-inlet-air temperature from 70° to 600° F. Sodium temperature varied from 800° to about 1100° F.

METHOD OF CALCULATION

Heat-Transfer Coefficient

Average heat-transfer coefficients were obtained for the air side of the shell-and-tube heat exchanger from the equation

$$h = \frac{\left[Wc_p(T_{in} - T_{out})\right]_{Na}}{S\theta_m}$$

(All symbols used herein are defined in appendix A.) The calculated heat transferred to the air averaged 8 percent above the heat given up by the sodium. Since the heat transferred cannot exceed the heat given up, the sodium heat loss was used in calculating average heat-transfer coefficients.

The log mean-temperature differential θ_m was calculated from the difference in sodium and air temperature at the inlet and outlet of the heat exchanger.

$$\theta_m = \frac{\theta_1 - \theta_2}{\ln \frac{\theta_1}{\theta_2}}$$

The inside tube-wall temperature was assumed to be equal to the sodium temperature. For the condition of the highest heat flux available, calculations showed that the temperature drop through the sodium film and tube wall would be in the order of 2° F, therefore, the error introduced would be negligible.

The physical properties of air, specific heat c_p and viscosity μ, were obtained from reference 1. A thermal conductivity k, that varies as the square root of the absolute temperature (ref. 2) was used. All properties of air used in calculating Nusselt, Prandtl, and Reynolds numbers were evaluated at an average film temperature T_f. The following

equation was used to define an average film temperature

$$T_f = \frac{T_s + T_b}{2}$$

Friction Factor

Shell-and-tube heat exchanger. - A diagram representing the air side of the shell-and-tube heat exchanger showing the stations used in calculating pressure follows:
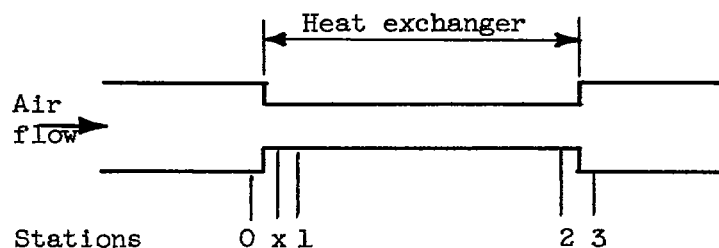
All instrumentation, consisting of total temperature, total pressure, and static pressure was located at positions 0 and 3.

The friction pressure drop, from station 1 to 2, was obtained from the experimental data by subtracting the momentum pressure drop from the static pressure drop.

$$\Delta p_{fr} = (p_1 - p_2) - \frac{G_1}{g}(V_2 - V_1)$$

$$= (p_1 - p_2) - \frac{RG_1^2}{g}\left(\frac{t_2}{p_2} - \frac{t_1}{p_1}\right)$$

where t_1 and t_2 are absolute static temperatures at stations 1 and 2. Static pressures p_1 and p_2 were calculated from recorded data taken at stations 0 and 3 by the following procedure:

Entrance losses: Because the Mach numbers at the inlet were less than 0.5, Bernoulli's equation was applied for the relation of total to static pressure in order to determine the static pressure at station 1.

$$P = p + \rho V^2/2g \tag{1}$$

The kinetic-energy term can be written in terms of temperature, pressure, and weight flow. Rewriting equation (1) yields

$$P = p + \frac{G^2 Rt}{2gp} \tag{2}$$

Static temperature may be evaluated from the following equation which was obtained from the general energy equation for a perfect gas.

$$t = -\frac{\gamma g p^2}{(\gamma - 1)RG^2} + \sqrt{\left[\frac{\gamma g p^2}{(\gamma - 1)RG^2}\right]^2 + 2T\left[\frac{\gamma g p^2}{(\gamma - 1)RG^2}\right]} \tag{3}$$

Substituting the expression for t of equation (3) into equation (2) and applying the assumption that the total pressure and total temperature remain constant from station 0 to 1, the following equation was used to determine the static pressure after the contraction:

$$p_x = \frac{P_0}{2\left(1 - \frac{\gamma - 1}{\gamma}\right)}\left[1 - \frac{2(\gamma - 1)}{\gamma} + \sqrt{1 - 4\left(1 - \frac{\gamma - 1}{\gamma}\right)\frac{RG_x^2 T_0}{2gP_0^2}}\right] \tag{4}$$

The vena contracta losses are taken as a factor C_c times the average velocity head at the entrance.

$$\Delta p_{vc} = C_c G_x^2 / 2g\rho_x \tag{5}$$

where C_c is a function of the free flow fraction of the heat exchanger and values are given in reference 3.

Subtracting equation (5) from (4) gives the static pressure at station 1.

$$p_1 = p_x - \Delta p_{vc}$$

Exit regain: The momentum change across the sudden expansion between stations 2 and 3 can be written as follows:

$$p_2 A_3 + \frac{W}{g} V_2 = p_3 A_3 + \frac{W}{g} V_3 \tag{6}$$

Applying equation (3) in conjunction with equation (6), the following relation for static pressure p_2 is obtained in terms of measured quantities of position 3.

$$\frac{p_2}{p_3} = \frac{\left(F - \frac{\gamma-1}{\gamma}\right)\left[\frac{t_3 R\left(\frac{G}{p}\right)_3^2}{g} + 1\right] + \sqrt{\left(F - \frac{\gamma-1}{\gamma}\right)^2\left[\frac{t_3 R\left(\frac{G}{p}\right)_3^2}{g} + 1\right]^2 + 4\left(F - \frac{\gamma-1}{2\gamma}\right)\left[\frac{\gamma-1}{2\gamma} - \frac{t_3 R\left(\frac{G}{p}\right)_3^2}{g}\left(1 - \frac{\gamma-1}{\gamma}\right)\right]}}{2\left(F - \frac{\gamma-1}{2\gamma}\right)} \quad (7)$$

Total temperature T_2 was assumed to be equal to total temperature T_3.

The average half friction factor $f/2$ was calculated from the friction pressure drop by use of the conventional relation modified to a film basis

$$\Delta p_f = 2f_f \, \frac{L}{D} \, \frac{G_1^2}{\rho_{av}} \, \frac{T_b}{T_f}$$

where

$$f_f = f \, \frac{T_f}{T_b}$$

solving for $\dfrac{f_f}{2}$

$$\frac{f_f}{2} = \frac{\Delta p_f}{4L/D} \, \frac{\rho_{av}}{G_1^2} \, \frac{T_f}{T_b}$$

where

$$\rho_{av} = \frac{p_1 + p_2}{R(t_1 + t_2)}$$

Finned-tube heat exchanger. - The pressure-drop data for the finned-tube heat exchanger were calculated from equations developed for the shell-and-tube heat exchanger. The pressure and temperature at the centerline of the first row of tubes were calculated in two steps. Equation (4) was applied for the contraction due to the fins and then for the contraction at the tubes. Vena contracta loss due to the fins was accounted for. Outlet conditions at the last row of tubes were also calculated in two steps applying equation (7) for each expansion.

3914

back 2-CJ-H

RESULTS AND DISCUSSION

Shell-and-Tube Heat Exchanger

Data for the shell-and-tube heat exchanger were obtained for two degrees of sodium purity. The oxygen content of the sodium had a marked effect on the heat-exchanger heat-transfer characteristics.

Heat balance. - A heat balance for the runs with filtered sodium is shown in figure 4 where the heat given up by the sodium Q_{Na} is plotted against the heat transferred to the air Q_a. A 45° line is drawn to represent the ideal heat balance. The plot shows that the calculated heat transferred to the air exceeded the heat given up. The average deviation from the ideal line is about 8 percent.

Heat-transfer coefficient. - Heat-transfer coefficients were taken for two conditions of sodium purity. The first set was obtained for sodium having an oxygen content in excess of 0.50 percent and a second set of runs representing data for sodium having less than 0.02 percent oxygen.

Air heat-transfer data for sodium of relatively high oxygen content are presented in figure 5(a). The results are shown with the Nusselt number divided by the Prandtl number raised to the 0.4 power $Nu_f/(Pr_f)^{0.4}$ plotted against a modified Reynolds number $\rho_f V_b D/\mu_f$. The solid line represents the conventional single-tube correlation corrected for the L/D ratio (ref. 4).

$$Nu = 0.021 \, Pr^{0.4} \, Re^{0.8}\left[1 + \left(\frac{L}{D}\right)^{-0.7}\right]$$

The L/D ratio for the exchanger was 180 and therefore the equation can be reduced to

$$Nu = 0.0216 \, Pr^{0.4} \, Re^{0.8}$$

For inlet-air temperatures of less than 300° F the data fell off to horizontal lines with increasing Reynolds number. A similar trend may be noted for the higher inlet-air temperature. At the highest Reynolds numbers the data is beginning to fall away from the solid line. In order to determine the cause of this drop off in the heat-transfer coefficient, a sodium sampling unit, as described in reference 5 was employed. A sample of sodium taken from the sump tank showed that there was a relatively large amount of oxygen in the system.

Because the heat exchanger is one of the coldest components in the loop, it effectively becomes a cold trap. Sodium oxide precipitates out and collects in dead areas of the shell and therefore part of the heat-transfer area becomes ineffective. The higher the air flow the more oxide collects and further reduces the heat-transfer area with the resultant low heat-transfer coefficients.

The oxygen content was reduced from 0.50 to 0.02 percent by passing sodium through a 5-micron micrometallic filter. Additional heat-transfer runs were taken and the results are shown in figure 5(b). The data taken with filtered sodium agreed well with the recommended correlation and there was no leveling off of the heat-transfer coefficient for low inlet-air temperature. If the sodium is relatively free of oxygen the heat-transfer performance of a shell-and-tube heat exchanger can thus readily be predicted.

Friction-factor data. - The experimental friction-factor data with no heat addition for the shell-and-tube heat exchanger is shown in figure 6(a). Half friction factor $f_f/2$ is plotted against the Reynolds number $G_1 D/\mu$. Included for comparison is the Kármán-Nikuradse curve for the relation between friction factor and Reynolds number which is

$$\frac{1}{\sqrt{8\frac{f}{2}}} = 2 \log \left(Re \sqrt{8\frac{f}{2}} \right) - 0.8$$

The data agree with the recommended Kármán-Nikuradse line for the Reynolds numbers covered.

Friction-factor data taken with heat transfer is shown in figure 6(b). The data are also compared with the solid line representing the above equation. Half friction factor is plotted against a modified Reynolds number where all properties of air are evaluated at the film temperature. The data for Reynolds numbers greater than 30,000 lie about 10 to 20 percent below the solid line. The reason for this discrepancy cannot be explained. It should be noted that this area represents data of high exit Mach number and in some cases high heat flux.

Finned-Tube Heat Exchanger Friction Factor

Because of weld failures pressure-drop data for the finned-tube heat exchanger is limited to isothermal runs. Figure 7 shows the friction-factor data for five inlet-air temperatures. The aspect ratio of each passage is about 100 and L/D_e is about 440. The data of this investigation is compared with an analytical investigation (ref. 6) for flow between parallel plates. The experimental data fall about 55 percent above the solid line representing $f/2$ for parallel plates. The difference

in the experimental data and the solid line is apparently due to the interference effect of the tubes. A description of the failure of this heat exchanger and its possible cause is included in appendix B.

SUMMARY OF RESULTS

Heat-transfer and pressure-drop data were experimentally obtained for the air side of a liquid-metal to air shell-and-tube heat exchanger. Because of weld failures, data for a finned-tube exchanger were limited to isothermal pressure drop. The inlet-air temperature was varied from 70° to 600° F over a Reynolds number range of 7000 to 115,000. The sodium temperature ranged from 800° to 1100° F. The following results were obtained:

1. Air-side heat-transfer coefficients with filtered sodium correlated with conventional single-tube heat-transfer coefficients.

2. Because of oxide precipitation air-side heat-transfer data with sodium of high oxygen content fell below the recommended line for the lower inlet-air temperature.

3. Isothermal air-side friction-factor data for the shell-and-tube heat exchanger agreed with the Kármán-Nikuradse curve.

4. Air-side friction-factor data with heat transfer on the shell-and-tube heat exchanger fell about 10 to 20 percent below the recommended line at high Reynolds numbers but agree reasonably well at low Reynolds numbers.

5. The finned-tube isothermal air-side friction factor was 55 percent higher than theory predicts for flat plates which is probably due to tube interference.

Lewis Flight Propulsion Laboratory
    National Advisory Committee for Aeronautics
        Cleveland, Ohio, December 8, 1955

APPENDIX A

SYMBOLS

The following symbols are used in this report:

A   cross-sectional flow area, sq ft

C_c contraction coefficient

c_p specific heat, Btu/(lb)(°F)

D   inside diameter of tubes, ft

D_e equivalent diameter for finned-tube exchanger (twice the fin spacing), ft

F   free-flow fraction (ratio of minimum flow area to frontal area)

f   friction factor

G   mass flow per unit cross-sectional area, lb/(hr)(sq ft)

g   acceleration due to gravity, 4.17×10^8 ft/sq hr

h   average heat-transfer coefficient, Btu/(hr)(sq ft)(°F)

k   thermal conductivity, Btu/(hr)(sq ft)(°F/ft)

L   heat-transfer length, ft

Nu   Nusselt number, hD/k

P   absolute total pressure, lb/sq ft

Pr   Prandtl number, $c_p \mu / k$

p   absolute static pressure, lb/sq ft

Δp_{fr} friction static-pressure drop across heat exchanger, lb/sq ft

Δp_{vc} vena contracta pressure drop, lb/sq ft

Q_a heat absorbed by air, Btu/sec

Q_{Na} heat given up by sodium, Btu/sec

3914

R   gas constant for air, 53.3 ft-lb/(lb)($^{\circ}$F)

Re   Reynolds number, $\rho VD/\mu$, GD/μ

S   heat-transfer area, sq ft

T   total temperature, $^{\circ}$R

T_b average bulk temperature defined as $(T_1 + T_2)/2$, $^{\circ}$R

T_f average film temperature defined as $(T_s + T_b)/2$, $^{\circ}$R

T_s average inside surface temperature defined as the average sodium temperature, $^{\circ}$R

t   static temperature, $^{\circ}$R

V   velocity, ft/hr

W   rate of flow, lb/hr

γ ratio of specific heats of air

θ temperature difference between air and sodium, $^{\circ}$R

θ_m log mean temperature difference, $^{\circ}$R

μ absolute viscosity of air, lb/(hr)(ft)

ρ density, lb/cu ft

Subscripts:

a   air

av   average

b   bulk (when applied to properties, indicates evaluation at bulk temperature T_b)

f   film (when applied to properties, indicates evaluation at average film temperature T_f)

Na   sodium

x   station before vena contracta

0   station ahead of heat exchanger

1   station at exchanger inlet

2   station at exchanger outlet

3   station after heat exchanger

3914

APPENDIX B

FINNED-TUBE HEAT-EXCHANGER FAILURE

The finned-tube heat exchanger was thoroughly checked for leaks as described in the text. The exchanger was installed and isothermal air-side friction factor data were taken. After the initial runs were completed, sodium was circulated through the system to obtain data with heat addition. After only a few minutes of sodium flow the leak-detector alarm went off and shut down the system. The test section was removed and cleaned and a pressure check with air and water showed that 13 tubes leaked severely with only 5 pounds per square inch air pressure. The exchanger was sectioned and examined.

In order to understand more fully the method and cause of failure, the method of construction must be known. The two header plates and 77 fins were stacked and drilled as a unit in order to eliminate any mis-alinement of holes. The tubes were heliarc welded into one of the header plates as shown in the sketch below.

Before welding   After welding
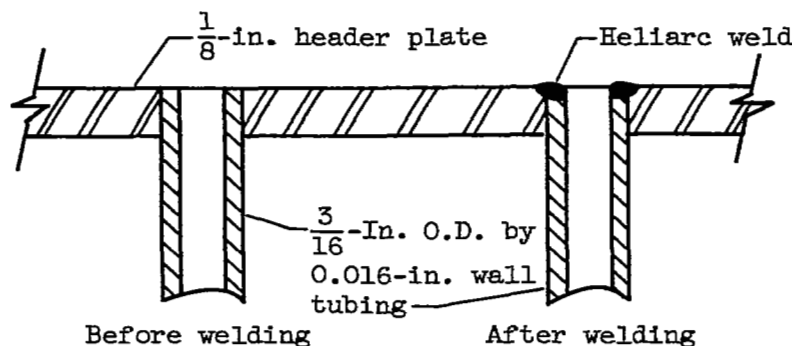
The fins were dimpled to provide spacing and pressed over the tubes. The other header plate was then welded and the other pieces of the exchanger were assembled.

After failure, the header cover plates were cut off exposing the ends of the tubes. The first obvious fault was that the tubes near each end were bowed outward toward the ends while the tubes near the center had remained straight. One of the bowed tubes is shown in figure 8(a). The end tubes were also bent sharply at the inner edge of the header plates as shown in figure 8. Close examination of figure 8(b) shows that actual failure occurred at the junction of the heliarc weld and the tube.

The one-piece fins apparently were the main factor contributing to the failure. The failure was probably caused by the rapid heating of the fins relative to the header plates which bowed the tubes and simultaneously drew the tubes from the headers. An unexplained fact is that the fins remained elongated relative to the header plates after cooling. This may be due to the relief of internal stresses in the fins from the dimpling process.

REFERENCES

1. Keenan, Joseph H., and Kaye, Joseph: Thermodynamic Properties of Air. John Wiley & Sons, Inc., 1945.

2. Humble, Leroy V., Lowdermilk, Warren H., and Desmon, Leland G.: Measurements of Average Heat-Transfer and Friction Factor Coefficients for Subsonic Flow of Air in Smooth Tubes at High Surface and Fluid Temperatures. NACA Rep. 1020, 1951. (Supersedes NACA RM's E7L31, E8L03, E50E23 and E50H23.)

3. McAdams, William H.: Heat Transmission. Second ed., McGraw-Hill Book Co., Inc., 1942.

4. Weiland, Walter F., and Lowdermilk, Warren H.: Measurements of Heat-Transfer and Friction Coefficients for Air Flowing in a Tube of Length-Diameter Ratio of 15 at High Surface Temperatures. NACA RM E53E04, 1953.

5. Lyon, Richard N., ed.: Liquid-Metals Handbook. Second ed., Atomic Energy Comm., Dept. Navy, June 1952.

6. Deissler, Robert G.: Analysis of Turbulent Heat Transfer and Flow in the Entrance Regions of Smooth Passages. NACA TN 3016, 1953.

Fuel burner

Heat exchanger

Electric resistance heater

Coaxial
bus bar

Volume
measuring
tank

500 kw
25 v
20,000 amps

Reactor   Transformer

Pump and   Variable
sump tank   speed motor
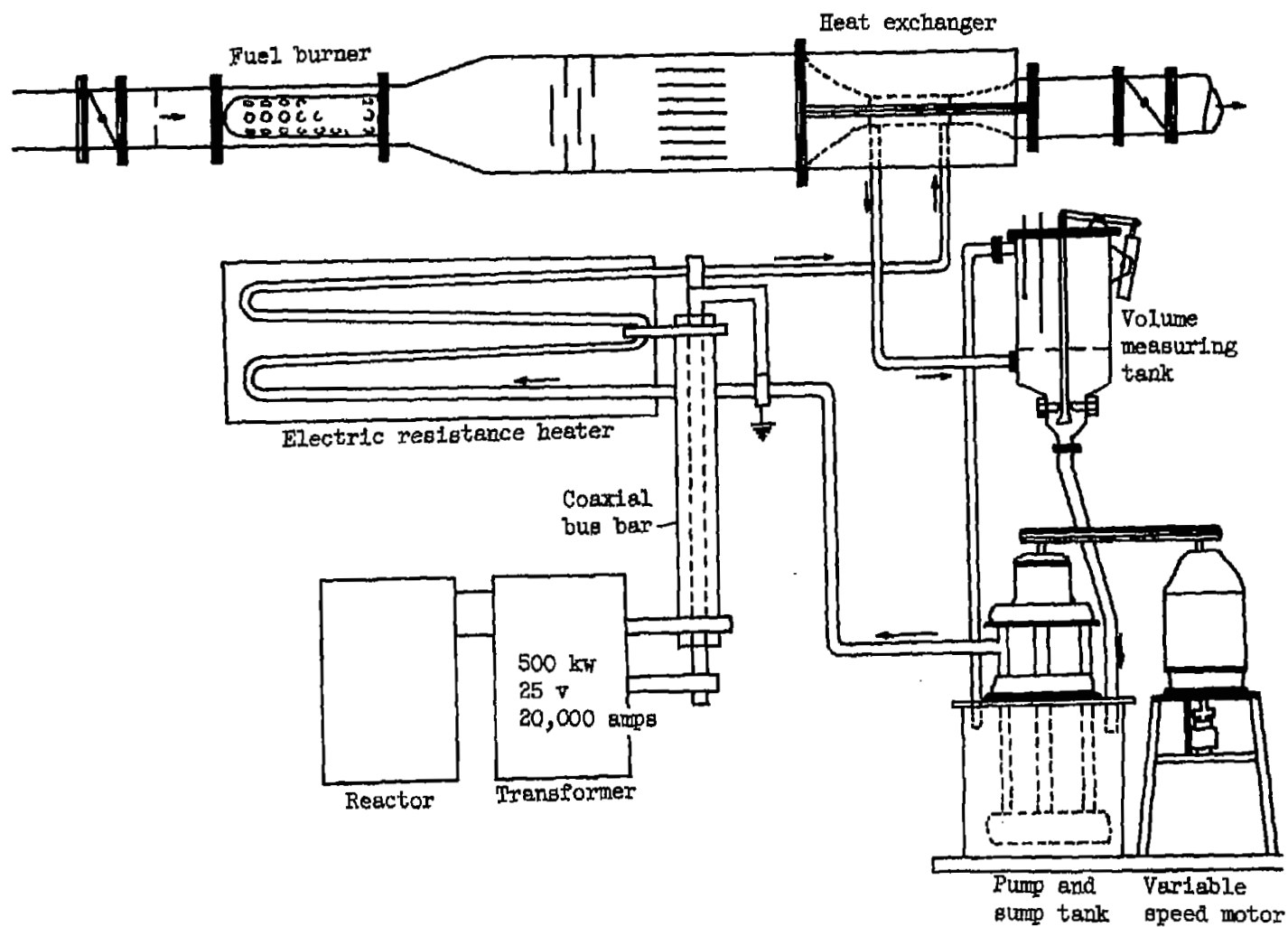
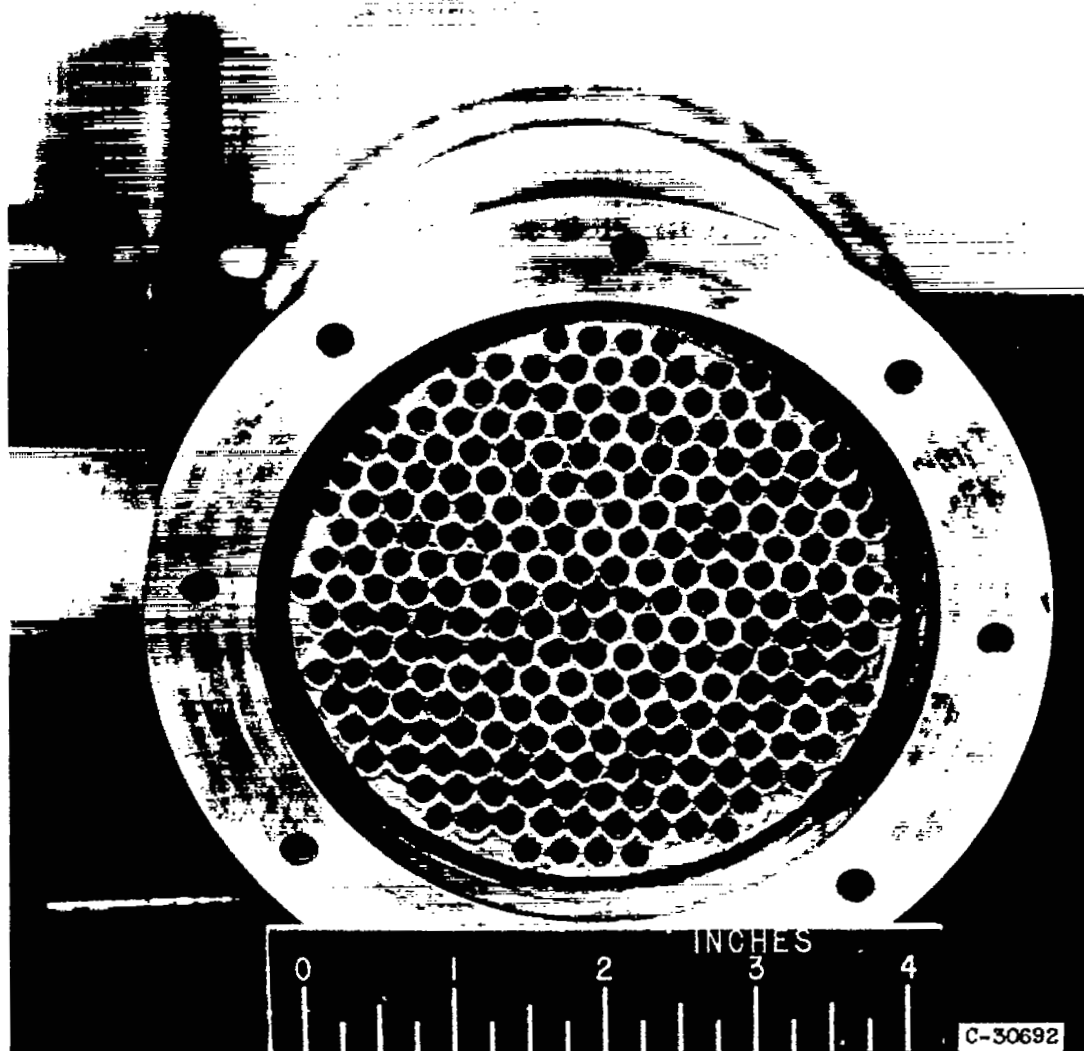Figure 1. - Schematic drawing of 500-kilowatt liquid-metal heat-exchanger test facility.

28"

4.25"

Air flow

241 Tubes

Sodium flow

$\frac{3}{16}$-In. O.D. tubing by 0.016 wall

$\frac{1}{4}$"

$\frac{1}{4}$"

CD-4782
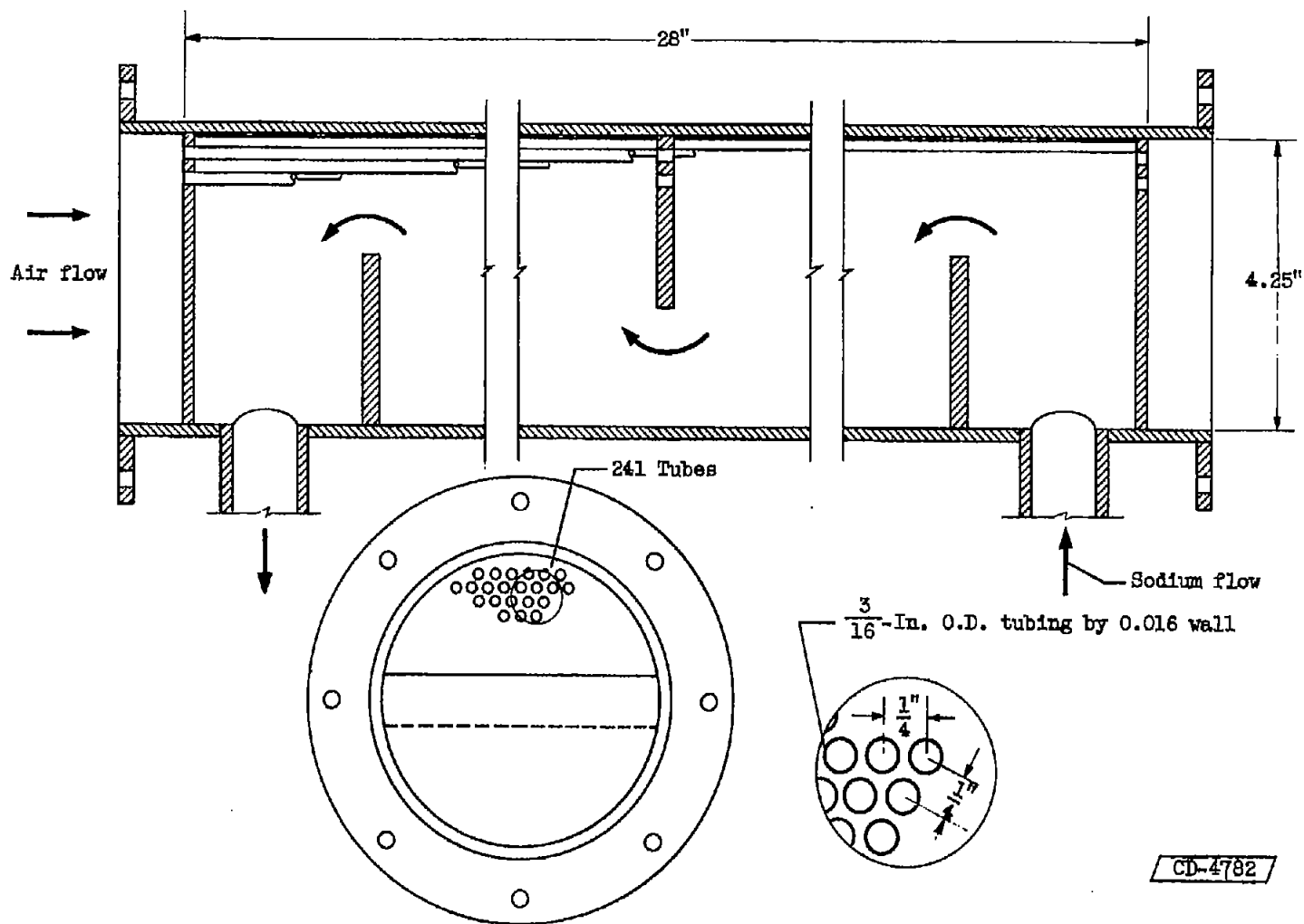
(a) Cross section.

Figure 2. - Shell-and-tube heat exchanger.
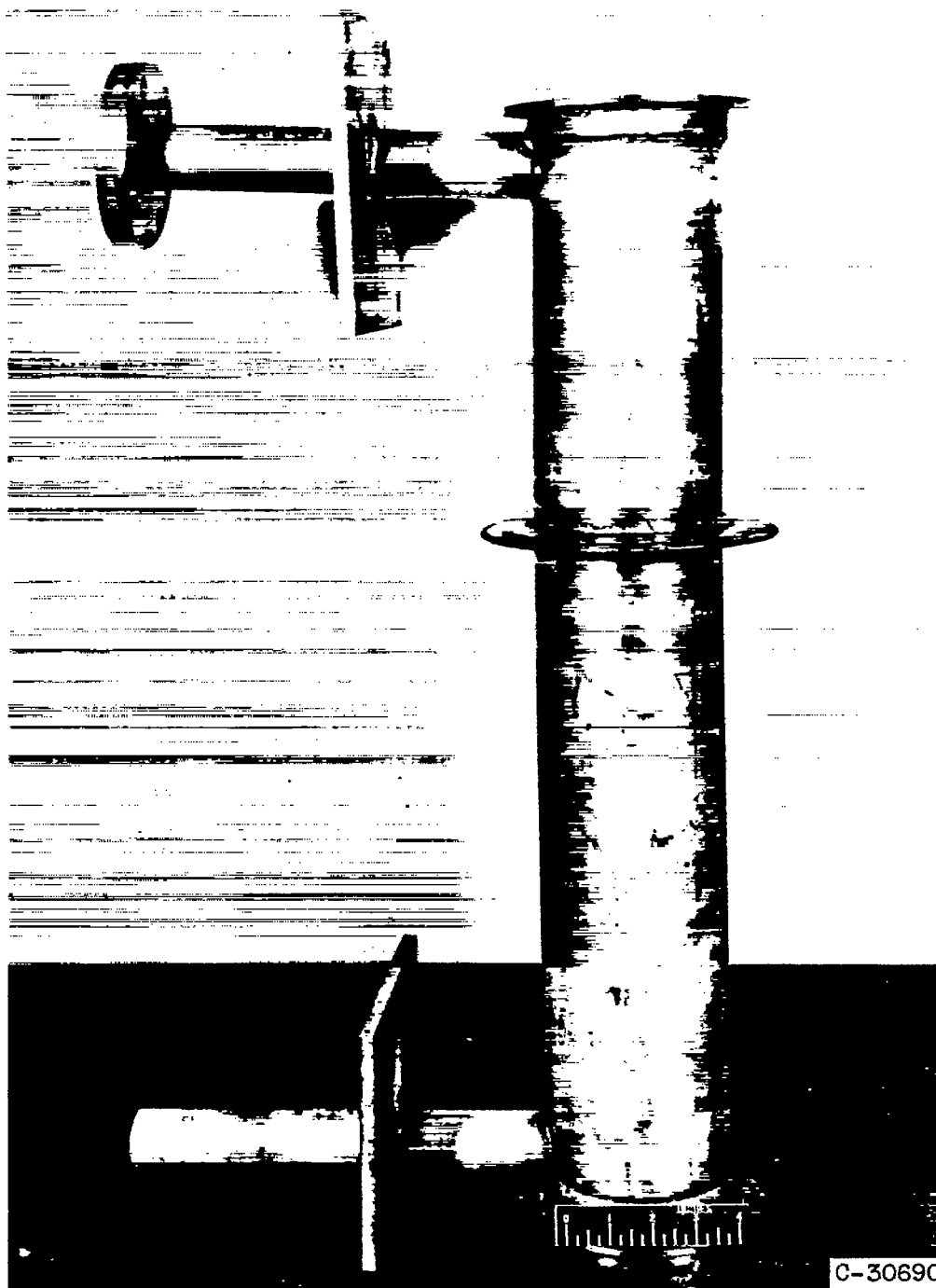
(b) Side view of completed heat exchanger.

Figure 2. - Continued. Shell-and-tube heat exchanger.

(c) End view showing 241 tubes welded to header plate.

Figure 2. - Concluded. Shell-and-tube heat exchanger.

29"

Air flow

4.00"
by
3.28" wide

Sodium flow

CD-4783

0.020"

77 Fins; 28 in. long by 0.020 in. thick
102 Tubes; 3/16-in. O.D. by 0.016-in. wall
3 Tubes and 1 half round per bank
Fins are dimpled and forced over tubes
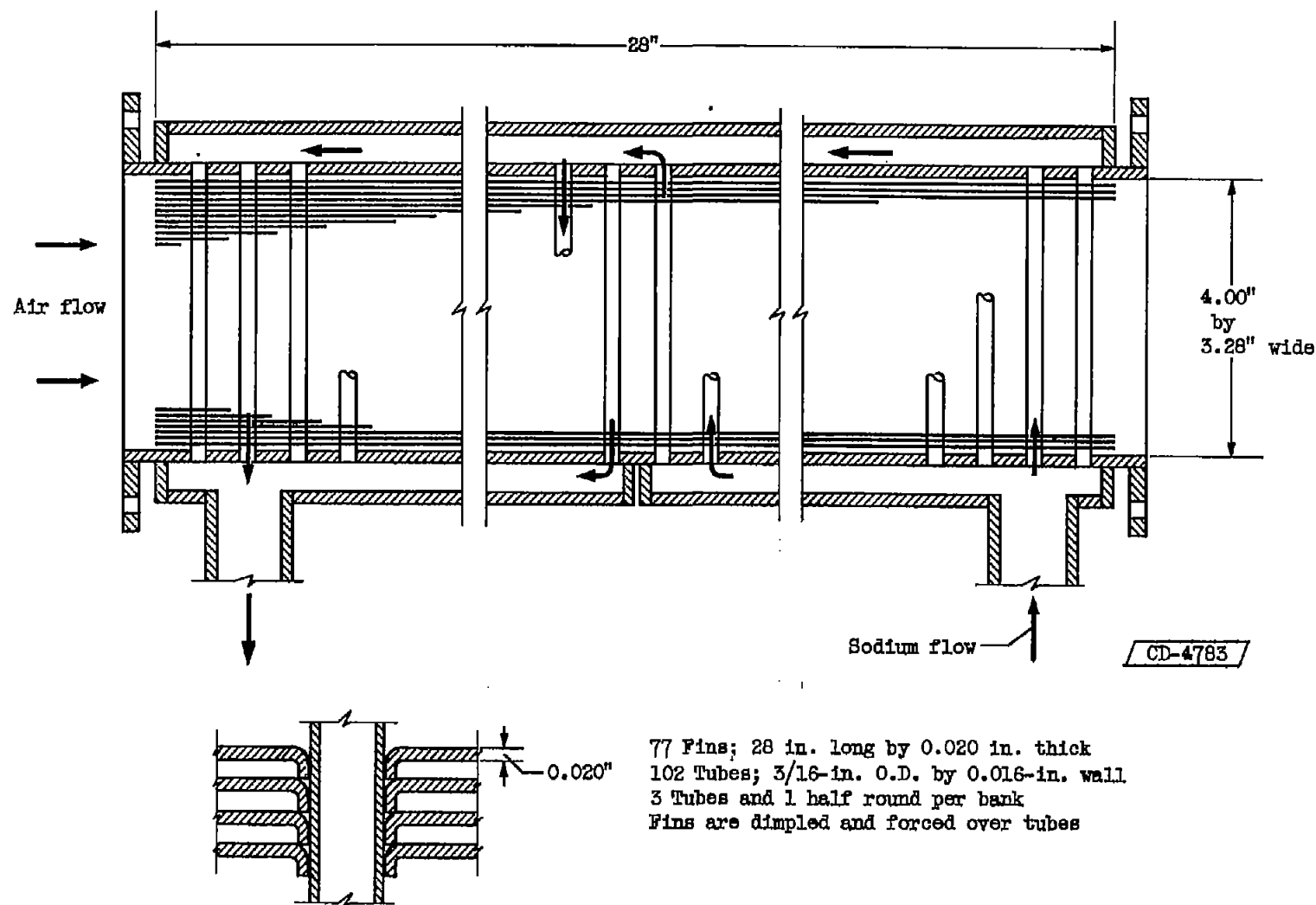
(a) Cross section.

Figure 3. - Finned-tube heat exchanger.
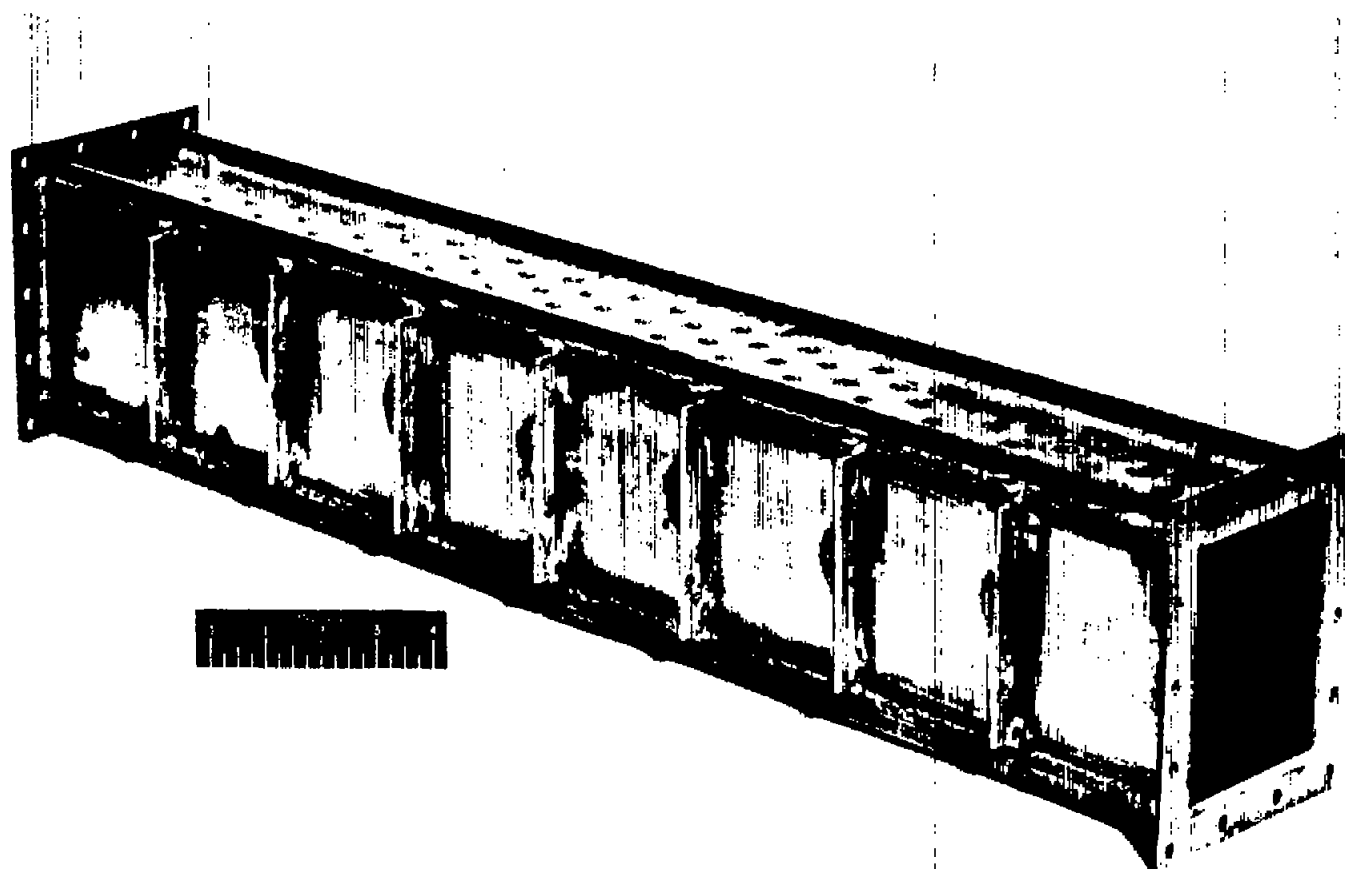
C-34644

(b) Heat exchanger without header covers.

Figure 3. - Continued. Finned-tube heat exchanger.
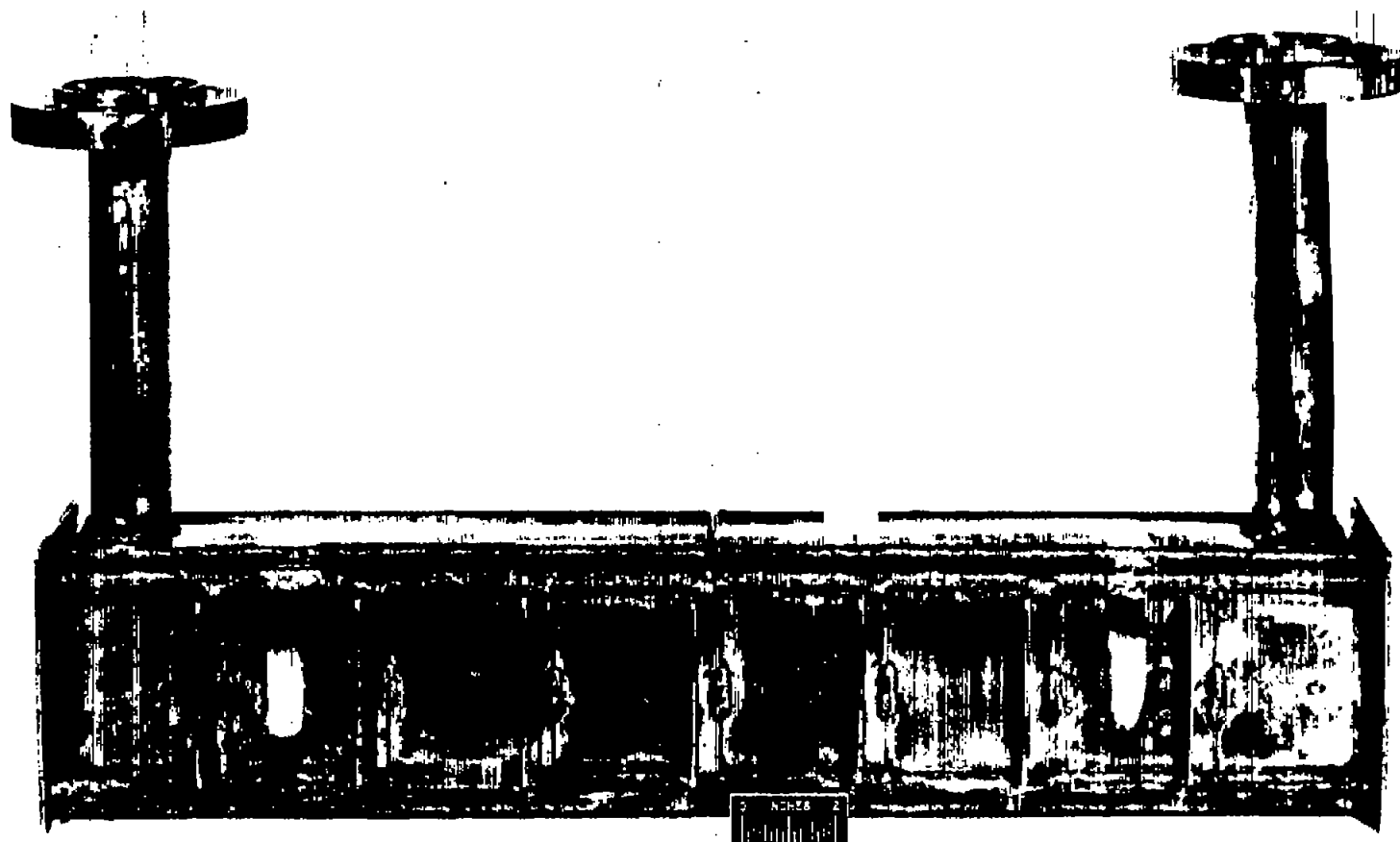
C-38176

(c) Side view of completed heat exchanger.

Figure 3. - Continued. Finned-tube heat exchanger.
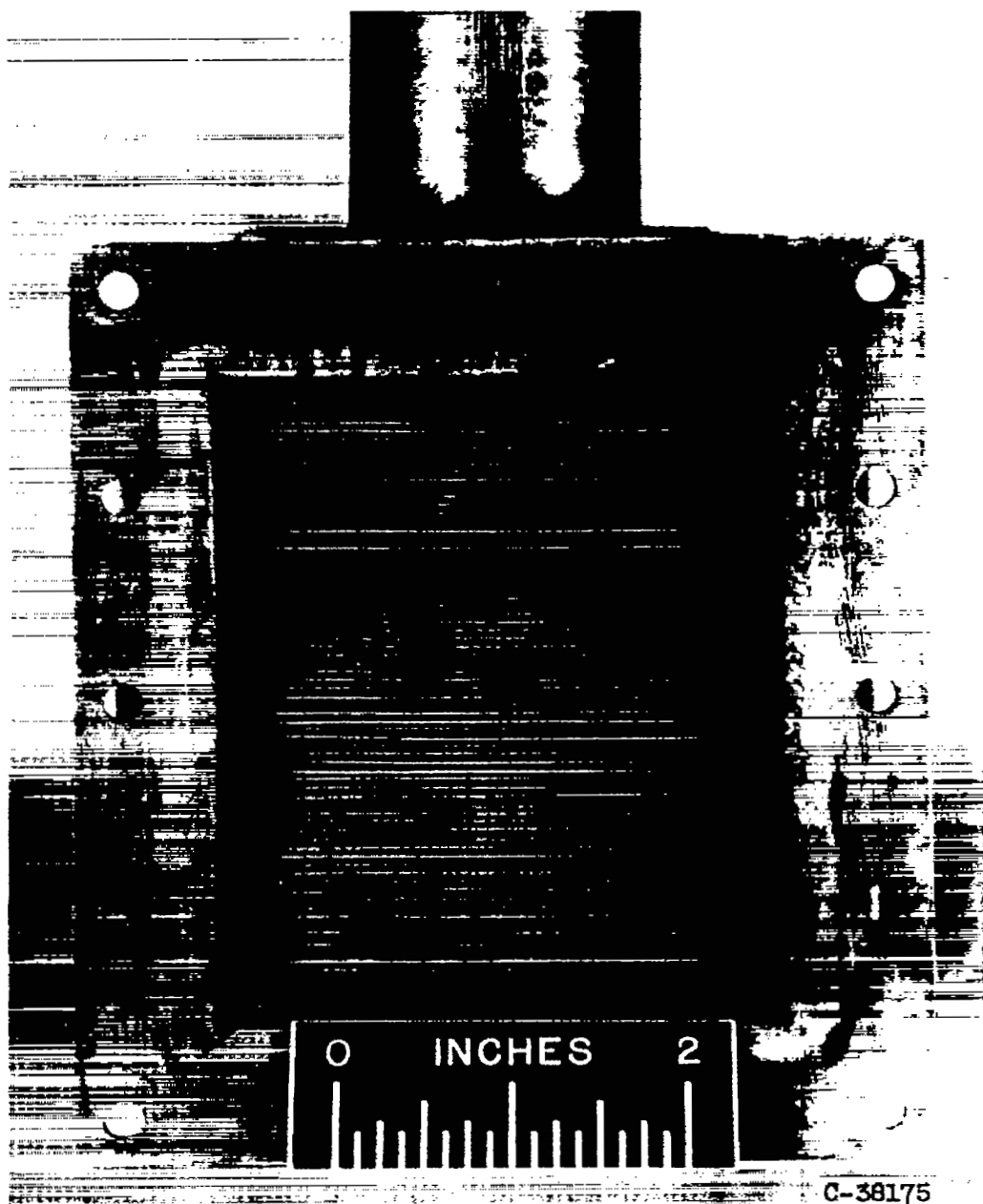
(d) End view of heat exchanger.

Figure 3. - Concluded. Finned-tube heat exchanger.

3914

CF-4 back
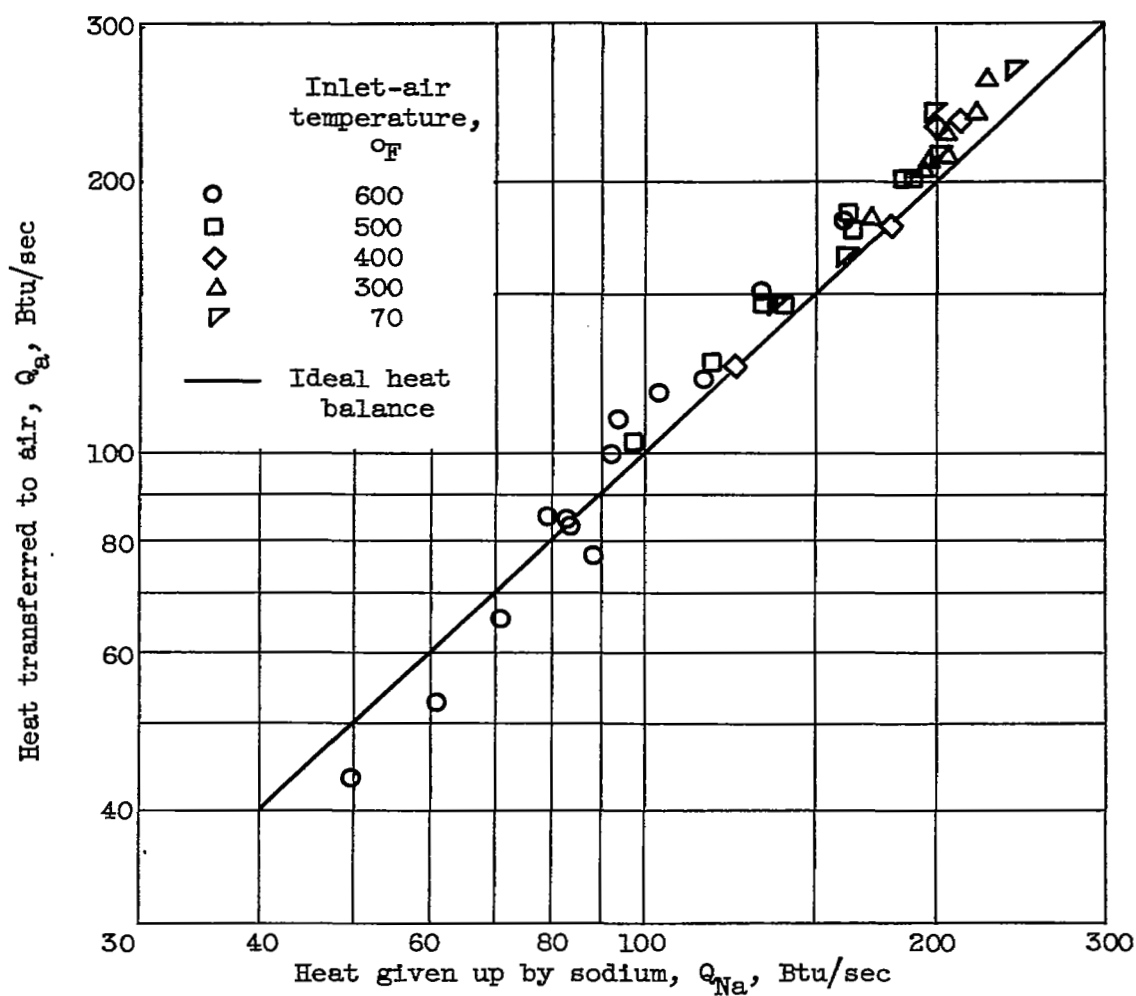
Figure 4. - Heat balance.
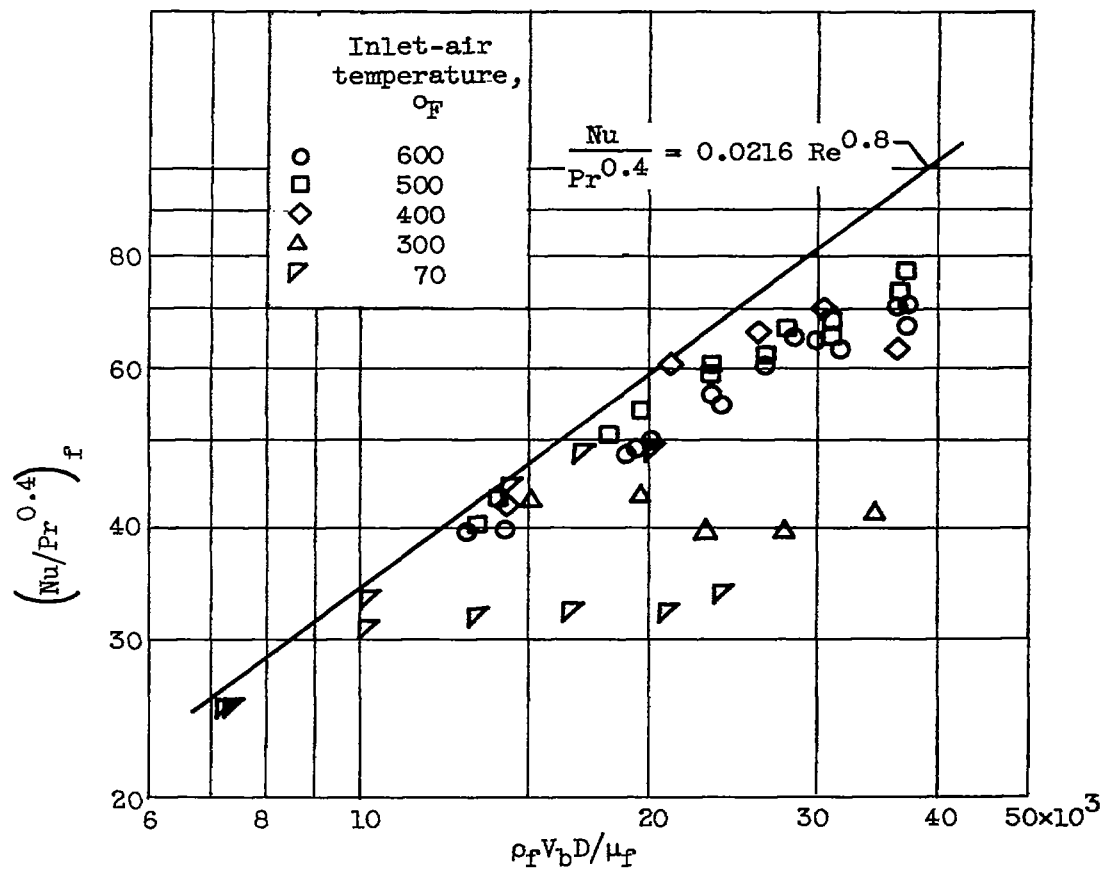
(a) Prior to filtering of sodium.

Figure 5. - Heat-transfer data.

3914
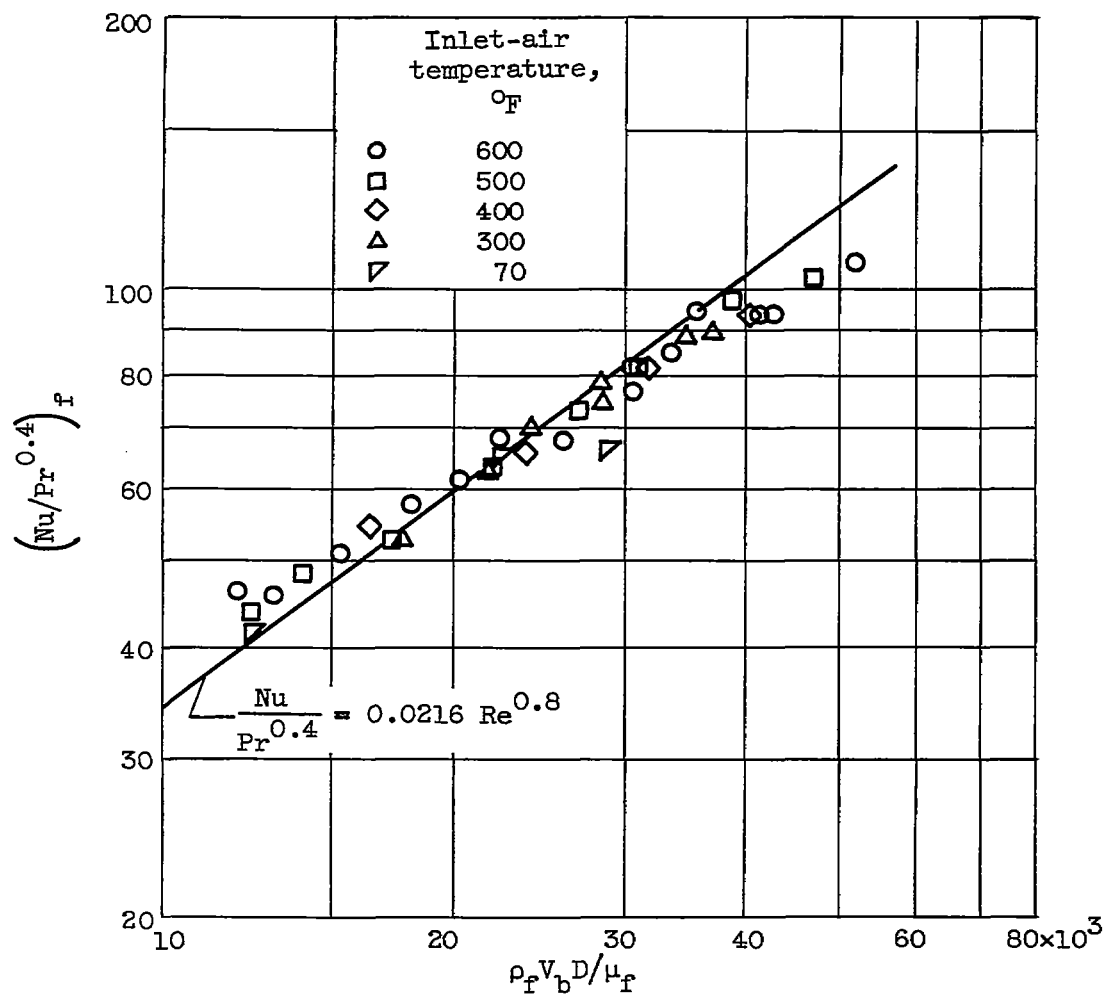
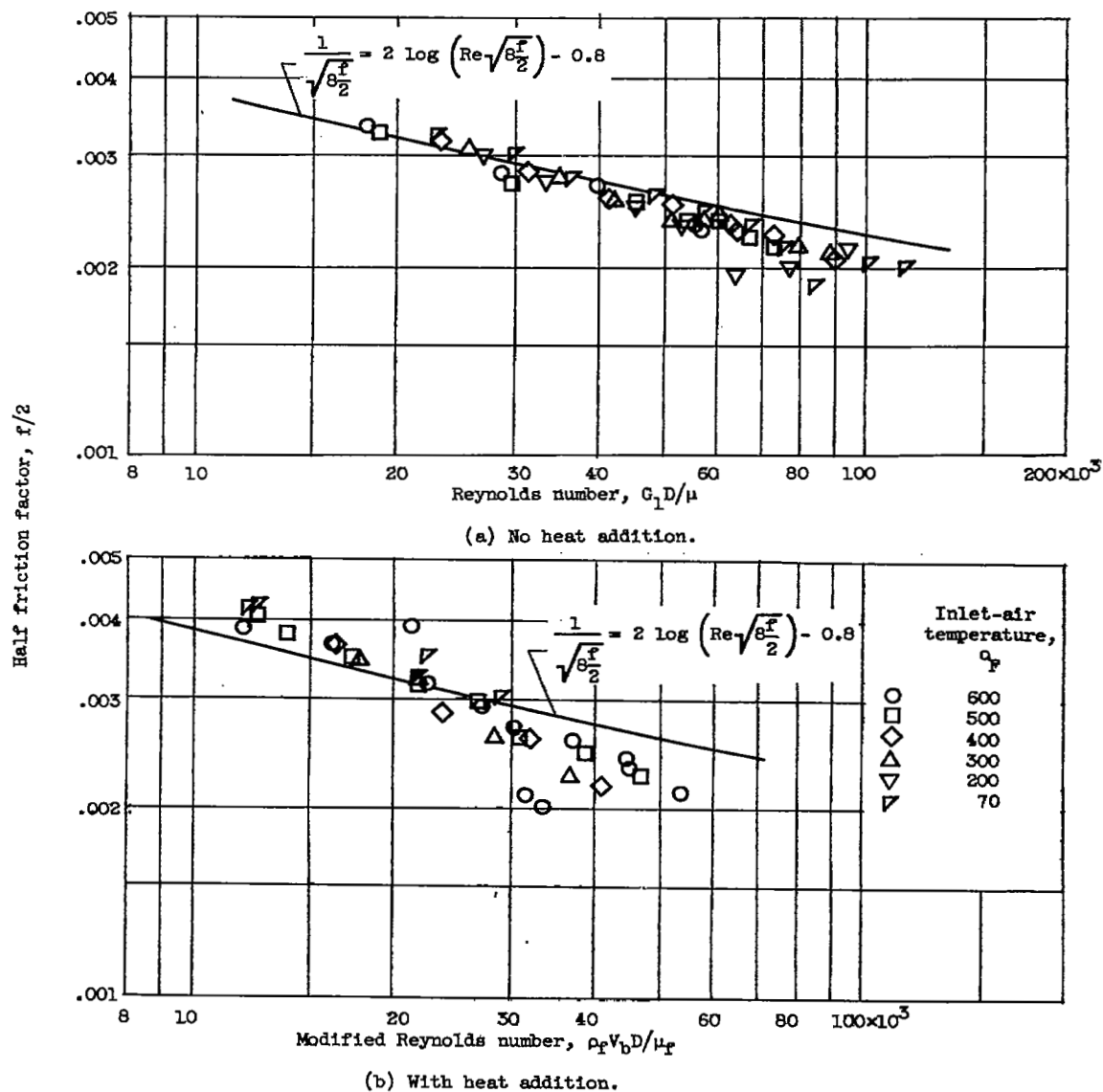(b) With filtered sodium.

Figure 5. - Concluded. Heat-transfer data.

(a) No heat addition.

(b) With heat addition.

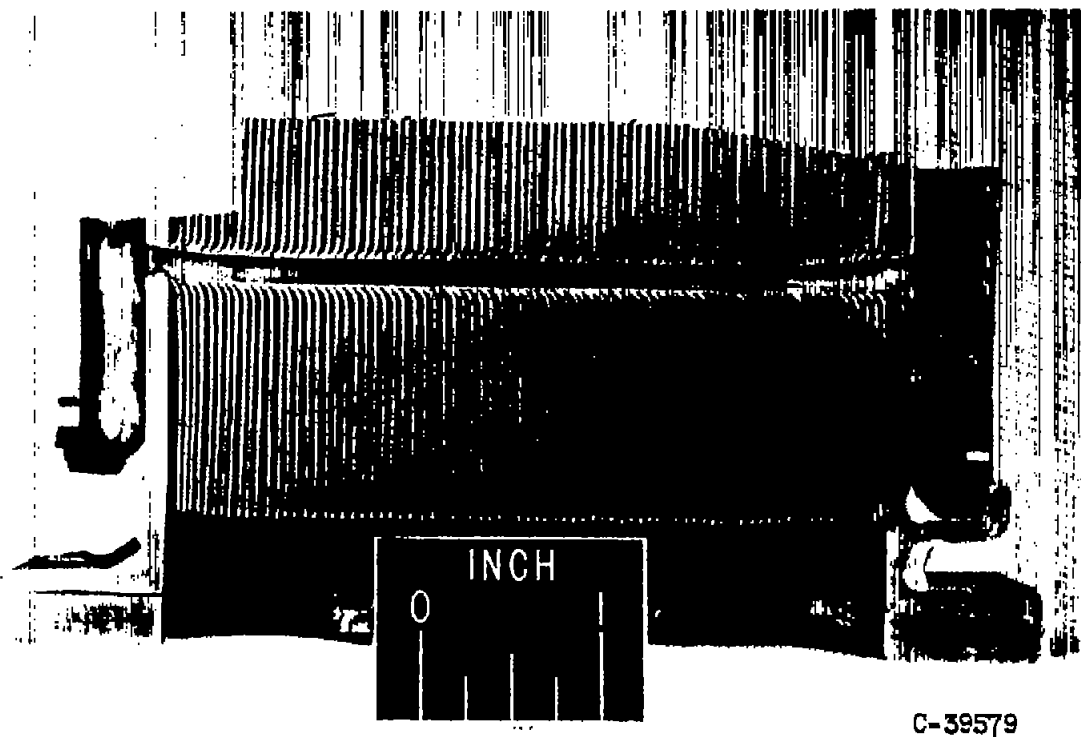Figure 6. - Friction factor for shell-and-tube heat exchanger.
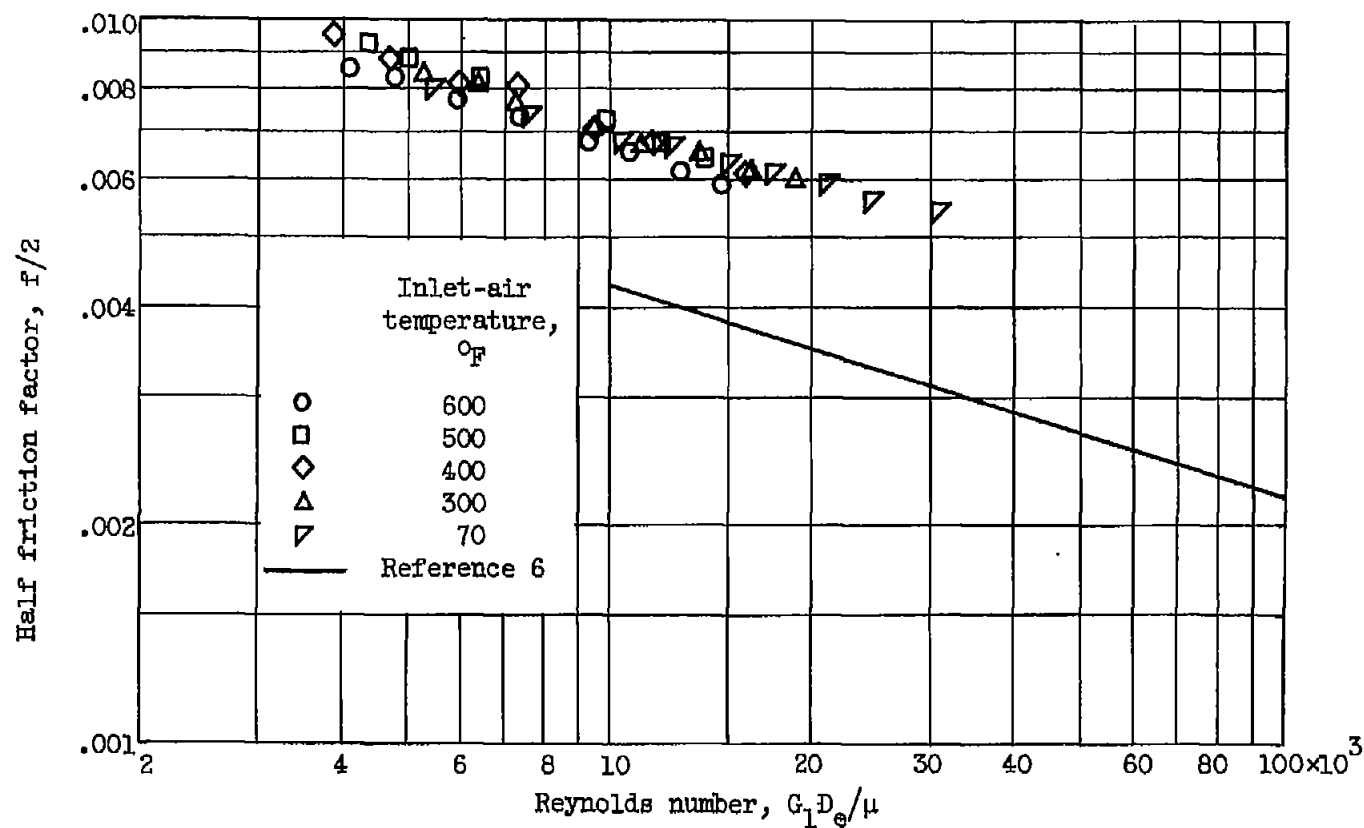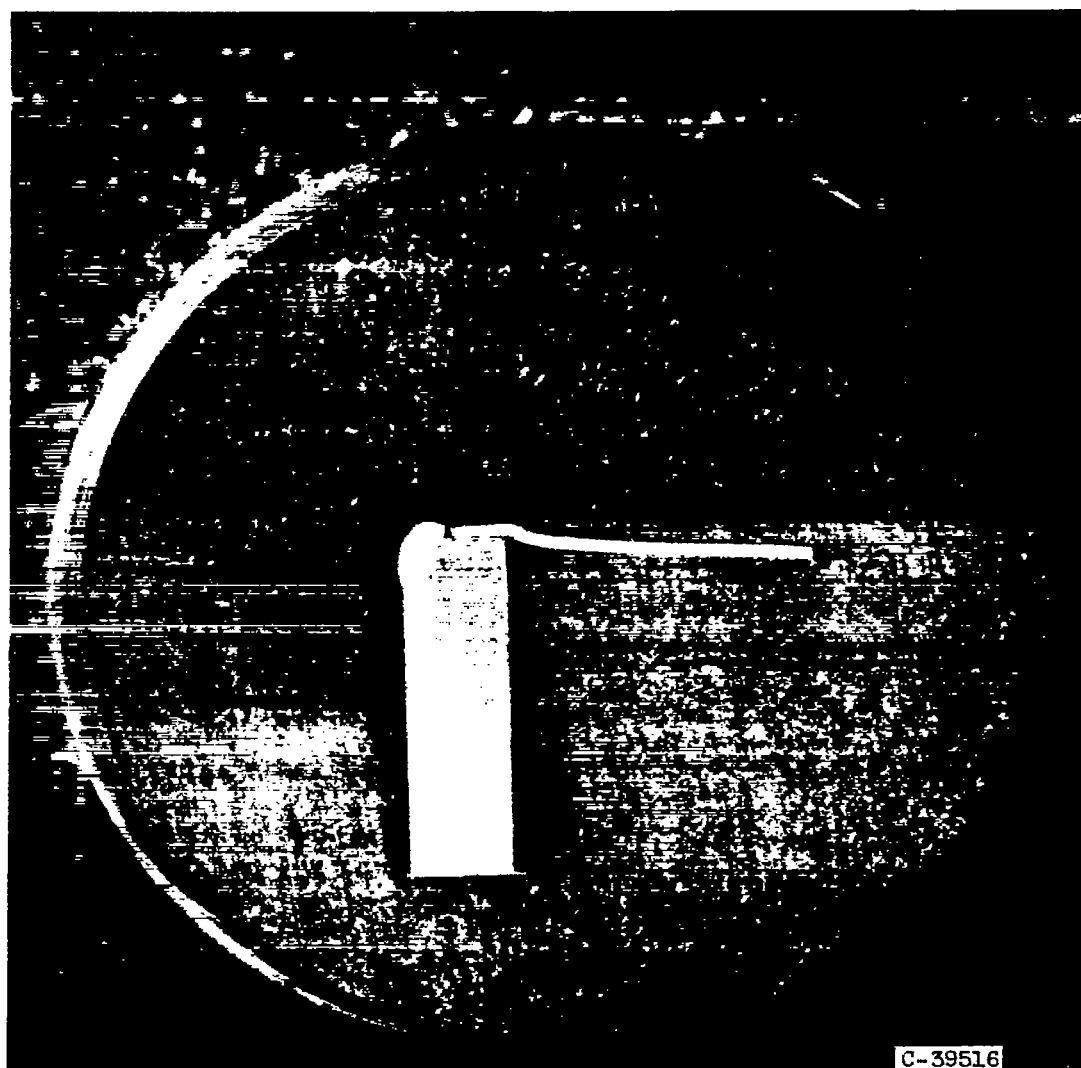
Figure 7. - Friction factor for finned-tube heat exchanger with no heat addition.

C-39579

(a) Cross section of one tube near end of heat exchanger.

Figure 8. - Section of finned-tube heat exchanger.

(b) Tube-to-header joint. 3/16-Inch O.D. by 0.016-inch
wall tube to 1/8-inch header plates. (5X.)

Figure 8. - Concluded. Section of finned-tube heat exchanger.